150 mW/π, which means the total power consumption of the equaliser is at most 4.5 W when obtaining an arbitrary filtering waveform.

Next, we examined the gain flattening characteristics for an EDTFA Fig. 2 shows raw and equalised spectra for the ASE of the EDTFA. The ASE spectrum is flattened over a 68 nm wavelength range with a 0.9 dB ripple. We set the power of each phase shifter to achieve a flat condition. By using the polarisation diversity system, the polarisation dependent loss (PDL) of the equaliser was successfully suppressed from 3.5 to 0.5 dB at 1560 nm where the highest attenuation was achieved. The residual 0.5 dB PDL was mainly considered to result from the misalignment of the PMF and waveguide polarisation axes. While the base FSR of the equaliser was designed to be 80 nm which corresponds to the maximum equalising range, the equalisation range in our experiment was reduced to 68 nm. This is because the Fourier transformation loss of the equaliser is increased drastically if the equalising range is close to its maximum value. So, we chose an equalisation range of 68 nm with a Fourier transformation loss of 1 dB.

The insertion loss of the equaliser was 9 dB, and consisted of fibre coupling loss (3 dB), waveguide propagation loss (2 dB), Fourier transformation loss (1 dB), and the loss of the polarisation diversity device (3 dB). Although the SHΔ PLC has a relatively high fibre coupling loss, this can be suppressed to 0.5 dB by using spotsize converters [8]. The loss caused by the polarisation diversity configuration will also be less than 2 dB if we optimise the devices used. Therefore, we estimate that the total insertion loss will be 5.5 dB after optimisation.

Conclusion: We have described a PLC-based wideband dynamic gain equaliser that covers the C- and L-bands. The equaliser consists of 10 cascaded Fourier series MZIs with an 80 nm base free spectral range. Using an SHΔ PLC we were able to design a compact equaliser with this configuration. We employed the equaliser to obtain gain flattening for an EDTFA spectrum and realised a residual ripple of 0.9 dB over a 68 nm wavelength range. These results show that the PLC-type equaliser has the advantages of good controllability and excellent optical performance.

 17 May 2002
Electronics Letters Online No: 20020709
DOI: 10.1049/el:20020709

K. Suzuki, T. Kitoh, S. Suzuki, Y. Inoue, Y. Hibino, T. Shibata, A. Mori and M. Shimizu (*Photonics Laboratories, NTT Corporation, 3-1 Morinosato Wakamiya, Atsugi-City, Kanagawa Pref. 243-0198, Japan*)

References

1 YAMADA, M., MORI, A., ONO, H., KOBAYASHI, K., KANAMORI, T., and OHISHI, Y.: 'Broadband and gain-flattened Er^{3+}-doped tellurite fibre amplifier constructed using a gain equaliser', *Electron. Lett.*, 1998, **34**, (4), pp. 370–371

2 MATSUDA, T., MURAKAMI, M., IMAI, T., SUZUKI, K.Y., and KITOH, T.: 'Ultra-broadband Raman-amplified transoceanic system with adaptive gain equalization'. SubOptic 2001, Kyoto, Japan, 2001, Paper PDP-4

3 INOUE, K., KOMINATO, T., and TOBA, H.: 'Tunable gain equalizer using a Mach-Zehnder optical filter in multistage fiber amplifiers', *IEEE Photonics Technol Lett.*, 1991, **3**, pp. 718–720

4 DOERR, C.R., CHANG, K.W., STULZ, L.W., PAFCHEK, R., GUO, Q., BUHL, L., GOMEZ, L., CAPPUZZO, M., and BOGERT, G.: 'Arrayed waveguide dynamic equalization filter with reduced insertion loss and increased dynamic range', *IEEE Photonics Technol. Lett.*, 2001, **13**, pp. 329–331

5 KIM, H.S., YUN, S.H., KIM, H.K., PARK, N., and KIM, B.Y.: 'Dynamic gain equalization of erbium-doped fiber amplifier with all-fiber acoustio-optic tunable filters'. OFC'98, San Jose, CA, USA, 1998, Paper WG4

6 OFFREIN, B.J., HORST, F., GERMANN, G.L., SALEMINK, H.W.M., and BEYELER, R.: 'Adaptive gain equalizer in high-index-contrast SiON technology', *IEEE Photonics Technol. Lett.*, 2000, **12**, pp. 504–506

7 HIBINO, Y.: 'High contrast waveguide device'. OFC-2001, Anaheim, CA, USA, 2001, Paper WB1

8 MIZUNO, T., KITOH, T., SAIDA, T., INOUE, Y., ITOH, M., SHIBATA, T., HIBINO, Y., and HIDA, Y.: 'Low-loss 1.5%Δ arrayed waveguide grating with narrow laterally tapered spotsize converter', *Electron. Lett.*, 2001, **37**, (24), pp. 1452–1454

40 GHz pulse generating source with less than 350 fs timing jitter

G.J. Spühler, M. Dymott, I. Klimov, G. Luntz,
L. Baraldi, I. Kilburn, P. Crosby, S. Thomas,
O. Zehnder, C.Y. Teisset, M. Brownell,
K.J. Weingarten, R. Dangel, B.J. Offrein,
G.L. Bona, O. Buccafusca, Y. Kaneko,
L. Krainer, R. Paschotta and U. Keller

A simple 40 GHz pulse source combining a fundamentally modelocked 10 GHz laser with a planar waveguide integrated time-division multiplexer is demonstrated. Pulse trains with >5 dBm average power and <350 fs rms timing jitter were achieved.

We have recently demonstrated a simple, compact Er:Yb:glass laser oscillator (ERGO) which produces a continuous train of picosecond pulses at repetition rates of up to 12.7 GHz, a centre wavelength of 1535 nm, pulsewidths between 2.5 and 20 ps, and an average output power of up to 50 mW [1]. These pulses are obtained using fundamental passive modelocking with an intracavity semiconductor saturable absorber mirror (SESAM) [2, 3]. This has the advantage that no microwave drive signal is required to produce pulses (only DC signals for driving the laser and controls). Previously, a diode-pumped solid-state laser, passively modelocked with a SESAM, has been synchronised to timing jitter values below 20 fs rms [4]. We demonstrate here that the 10 GHz ERGO laser has an rms timing jitter <350 fs measured on an optical sampling oscilloscope, and a corresponding 80 fs rms determined by integrated phase noise over a frequency span of 10 Hz to 1 MHz. One key factor for our low timing jitter is based on our approach of fundamental modelocking instead of harmonic modelocking (i.e. only one laser pulse per round-trip inside the cavity).

Pulse generating sources at 40 GHz and above are becoming increasingly important for telecom applications. Transmission systems at 40 GHz and higher are likely to use return-to-zero (RZ) pulse formats with soliton dispersion management techniques. Current RZ transmitters typically require two modulators: one modulator functions as a pulse carver, and the other operates as the data encoder. With higher pulse repetition rates, the CW power has to be increased to compensate for the increased loss of the high-repetition-rate pulse carver and to maintain the number of photons per bit. Furthermore, to make things even more challenging, dispersion managed soliton transmission requires both more average power and higher quality pulses (i.e. unchirped pulses with a very good extinction ratio) to be launched into the fibre compared to other traditional schemes. Fortunately, contrast ratio and the time-bandwidth-products of passively modelocked multi-GHz solid-state lasers are typically very good [1, 5, 6], much better than carved pulses from CW sources. This improves system signal-to-noise and allows further scaling to higher repetition rates through optical time-division multiplexing. Therefore, 40 GHz data transmission would greatly benefit from the availability of simple, compact, transform-limited optical pulse generators, which could eliminate the need for the high-power CW laser, the pulse carver modulator and the associated drive electronics to create the pulses. This would simplify system architecture, increase efficiency, and reduce cost.

Here we describe our results where we have demonstrated a 40 GHz pulse generating source by combining a 10 GHz, passively modelocked, phase-locked ERGO with a 4X time multiplexer realised in high-index contrast silicon oxynitride (SiON) planar waveguide technology [7]. This system generates pulse trains with 4–7 ps pulsewidths, average power exceeding 5 dBm, and with phase noise essentially unchanged from the 10 GHz ERGO (except for the normal 12 dB scaling factor for phase noise due to the increase in carrier frequency from 10 to 40 GHz). The clean, high-contrast pulses from the ERGO allows for this optical time-division multiplexing.

Rather than pursue traditional approaches using fibre to optically multiplex, the 10 GHz repetition rate (corresponding to 30 mm free-space propagation distance between pulses) has allowed us to construct a simple, miniature, passive, integrated time multiplexer device. This component was realised in SiON planar waveguides with a core to cladding index contrast of 3.3% that leads to a strong guiding of the mode. Bent waveguide structures with radii as low as 0.8 mm without noticeable radiation losses can be achieved [7]. This device (Fig. 1) consists of two cascaded Mach-Zehnder structures (MZIs) built by three directional couplers and two delay lines of 50 and 25 ps, respectively. Each of these two MZIs doubles the incoming pulse repetition rate (10 → 20 → 40 GHz). The compact device is 6 × 16 mm in area and shows nominal total device insertion loss of 6 dB. The peak-to-peak pulse power variation introduced by the time multiplexer is < 0.2 dB when operated within its design range.

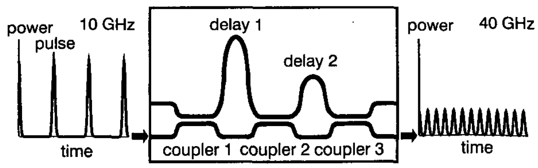

Fig. 1 *Schematic diagram of planar waveguide integrated time-division multiplexer*

Measuring the pulse train directly at 40 GHz is itself a technically challenging task. We can measure the microwave spectrum from a fast photodiode, which indicates sub-harmonic suppression at 10, 20, and 30 GHz of > 40 dB. This level of sub-harmonic suppression corresponds to either an amplitude variation of ~ 1% or a timing variation of ~ 0.25 ps rms, or some combination of both. It is difficult to measure optical autocorrelations in current commercial autocorrelator systems at 40 GHz. Time-domain measurements on state-of-art sampling oscilloscopes (DCA 86100A with 86109A 30/40 GHz plug-in) show essentially a sine-wave, since all higher harmonics of the pulse train are strongly filtered.

To obtain clean time-domain measurements, we used the recently introduced optical sampling oscilloscope system from Agilent Technologies (consisting of the DCA 86100A with 86119A optical sampler and 86107A precision timebase). This optically-based sampling system has a time resolution better than 0.5 ps and a timing jitter specification of better than 200 fs rms. This system has allowed us to resolve the time-domain pulse train and timing jitter, shown in Fig. 2.

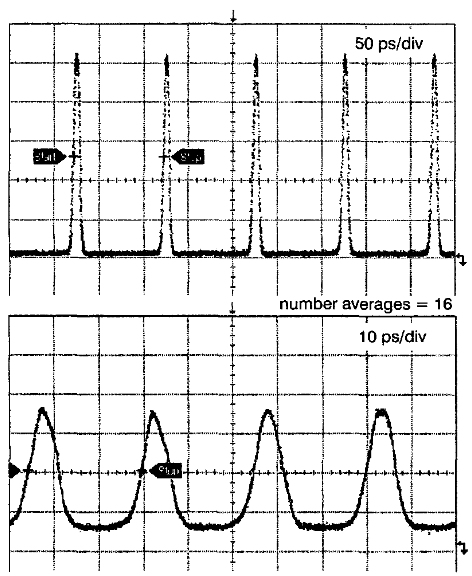

Fig. 2 *Pulse train (power against time) at 10 GHz (50 ps/div) and 40 GHz (10 ps/div) resolved with Agilent 86119A optical sampler*

It is well known that low-repetition rate (~ 100 MHz typically) passively modelocked lasers can be phase-locked to obtain excellent timing jitter stability [4]. The small physical size of the 10 GHz ERGO allows us to obtain very robust mechanical performance resulting in a very high performance 10 GHz phase-lock-loop feedback system using a low frequency loop bandwidth (< 100 kHz). Initial time-domain jitter measurements using the above mentioned optical sampler system have given timing jitter results of ~ 300–350 fs rms for the 10 GHz as well as for the 40 GHz pulse train. Corresponding phase noise measurements with a microwave spectrum analyser measured from 10 Hz to 1 MHz offset frequencies demonstrate phase noise which corresponds to an rms timing jitter of 80 fs for the 10 GHz ERGO laser and to 83 fs for the multiplexed signal (Fig. 3). Note that the nominal 12 dB increase in the phase noise from 10 to 40 GHz is due to the normal phase noise scaling factor $20\log(f_2/f_1)$ of the relative carrier frequencies f_1 and f_2 [8]. Thus, the rigid integrated planar waveguide multiplexer adds essentially no timing jitter in the addressed frequency domain. We are still investigating the discrepancy between the two measurements and believe it is related to the exact details of the measurement approaches. Note also that the phase noise of the 10 GHz ERGO is slightly increased relative to the low noise signal generator only in the 1–10 kHz regime.

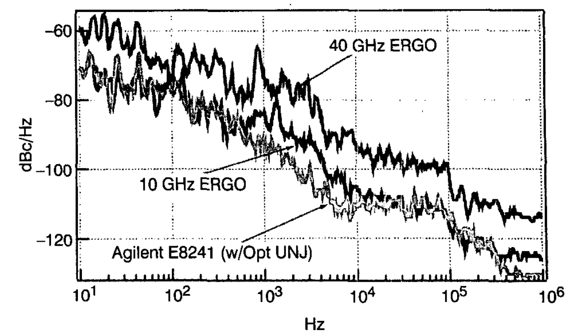

Fig. 3 *Phase noise power spectral density at 10 and 40 GHz showing 80 and 83 fs rms integrated timing jitter, respectively*

Conclusion: Passively SESAM modelocked lasers combined with a phase-locked loop feedback system and a planar lightwave circuit time-multiplexer can provide simple, compact, high-performance pulse generating sources for 40 GHz, featuring high average optical power and very low timing jitter. This approach also scales to 160 GHz and higher, limited by the ability to generate shorter optical pulses, and potential dispersion issues related to increasing bandwidth. In addition, the high-index contrast SiON waveguide technology is ideally suited for such time multiplexers owing to its ultra-small bending radius, which leads to compact devices.

28 May 2002
Electronics Letters Online No: 20020722
DOI: 10.1049/el:20020722

G.J. Spühler, M. Dymott, I. Klimov, G. Luntz, L. Baraldi, I. Kilburn, P. Crosby, S. Thomas, O. Zehnder, C.Y. Teisset, M. Brownell, K.J. Weingarten (*GigaTera, Inc., Lerzenstrasse 16, CH-8953, Dietikon, Switzerland*)

E-mail: gabriel.spuehler@gigatera.com

R. Dangel, B.J. Offrein and G.L. Bona (*IBM Research, Zurich Research Laboratory, Säumerstr. 4, CH-8803, Rüschlikon, Switzerland*)

O. Buccafusca and Y. Kaneko (*Agilent Technologies, Inc., 3910 Brickway Boulevard, Santa Rosa, CA 95403, USA*)

L. Krainer, R. Paschotta and U. Keller (*Ultrafast Laser Physics, Institute of Quantum Electronics, Swiss Federal Institute of Technology, ETH Hönggerberg - HPT, CH-8093, Zurich, Switzerland*)

References

1 KRAINER, L., PASCHOTTA, R., SPÜHLER, G.J., KLIMOV, I., TEISSET, C., WEINGARTEN, K.J., and KELLER, U.: 'Tunable picosecond pulse-generating laser with a repetition rate exceeding 10 GHz', *Electron. Lett.*, 2002, **38**, pp. 225–226

2 KELLER, U., MILLER, D.A.B., BOYD, G.D., CHIU, T.H., FERGUSON, J.F., and ASOM, M.T.: 'Solid-state low-loss intracavity saturable absorber for Nd:YLF lasers: an antiresonant semiconductor Fabry-Perot saturable absorber', *Opt. Lett.*, 1992, **17**, pp. 505–507

3 KELLER, U., WEINGARTEN, K.J., KÄRTNER, F.X., KOPF, D., BRAUN, B., JUNG, I.D., FLUCK, R., HÖNNINGER, C., MATUSCHEK, N., and AUS DER AU, J.: 'Semiconductor saturable absorber mirrors (SESAMs) for femtosecond to nanosecond pulse generation in solid-state lasers', *IEEE J. Sel. Top. Quantum Electron.*, 1996, **2**, pp. 435–453

4 TSUCHIDA, H.: 'Pulse timing stabilization of a mode-locked Cr:LiSAF laser', *Opt. Lett*, 1999, **24**, pp. 1641–1643
5 KRAINER, L., PASCHOTTA, R., MOSER, M., and KELLER, U.: '77 GHz soliton modelocked Nd:YVO_4 laser', *Electron. Lett.*, 2000, **36**, pp. 1846–1848
6 KEMP, A.J., STORMONT, B., AGATE, B., BROWN, C.T.A., KELLER, U., and SIBBETT, W.: 'Gigahertz repetition-rate from directly diode-pumped femtosecond Cr:LiSAF laser', *Electron. Lett.*, 2001, **37**, pp. 1457–1458
7 GERMANN, R., SALEMINK, H.W.M., BEYELER, R., BONA, G.L., HORST, F., MASSAREK, I., and OFFREIN, B.J.: 'Silicon oxynitride layers for optical waveguide applications', *J. Electrochem. Soc.*, 2000, **147**, pp. 2237–2241
8 KELLER, U., LI, K.D., RODWELL, M.J.W., and BLOOM, D.M.: 'Noise characterization of femtosecond fiber Raman soliton lasers', *IEEE J. Quantum. Electron.*, 1989, **25**, pp. 280–288

Tunable and switchable dual wavelength lasers using optical fibre Bragg grating external cavities

S.P. Reilly, S.W. James and R.P. Tatam

Two novel external cavity lasers are demonstrated experimentally. The first utilises a Bragg grating fabricated in highly birefringent optical fibre and offers the ability to switch between modes that are separated in polarisation and wavelength. The second utilises two spatially separate Bragg gratings fabricated in mono-mode fibre. Both can be used for tunable beat frequency generation.

Introduction: Fibre Bragg grating (FBG) external cavity semiconductor lasers have been investigated as stabilised continuous wave and modulated laser sources, and as tunable sources [1]. These lasers can offer narrow linewidths and a viable cost-effective alternative to distributed feedback laser diodes and distributed Bragg reflector laser diodes. Dual wavelength lasers have also been the subject of considerable research interest as sources capable of producing beat signals at microwave frequencies, which is desirable for electronic signal processing systems [2–4]. Beat frequencies have been generated previously using separate laser cavities [3, 4]. However, systems employing separate cavities can suffer from phase noise and drift, making a single cavity dual wavelength laser preferable for producing stable beat frequencies. In this Letter two novel FBG external cavity lasers are experimentally demonstrated. Both use the light reflected from the FBGs to force the lasers to operate at the Bragg wavelengths.

Hi-Bi laser: The first laser configuration considered is based on high birefringence (Hi-Bi) fibre and exploits the difference in the wavelength of the Bragg reflection of light populating the orthogonally linearly polarised eigenaxes of Hi-Bi fibre. Feedback from a FBG written in Hi-Bi fibre then results in the laser operating on two linearly polarised longitudinal modes that are separated in both wavelength and polarisation. An Hi-Bi fibre with a beat length of ~1.6 mm will produce a corresponding wavelength separation of ~0.3 nm between the orthogonally linearly polarised modes of the reflection from the FBG. The fibre used was Fibercore bow-tie (HB 750) with a numerical aperture of 0.15. The fibre was hydrogen loaded for seven days in a pressure vessel at 130 bar. The FBG was subsequently fabricated using a wavelength tunable UV source and phase mask based interferometer [5]. The FBG had a centre wavelength of 810 nm, a reflectivity of ~40% and a bandwidth of 0.15 nm (FWHM) and was located 250 mm from the end of the fibre. The fibre end was angle polished to reduce unwanted reflections into the active laser cavity that could destabilise the laser. Light was coupled into the fibre using antireflection (AR) coated lenses. The output from a 150 mW, SDL 5420, non-AR coated 810 nm laser diode was coupled into the angle polished end of the fibre. A coupling efficiency of ~40% was achieved. The optical length of the external cavity was ~320 mm. A half wave plate was used to adjust the orientation of the polarisation of light with respect to the eigenmodes of the fibre. Tuning of the wavelength separation between the modes was demonstrated by transversely loading the FBG [6]. This altered the birefringence, via the strain-optic effect, of the fibre at the location of the FBG, altering the wavelength separation of the two modes. A series of weights were used to apply a transverse load to the fibre. The weights were placed on a glass slide positioned on the FBG parallel to another fibre of the same type that also had its coating removed. Applying the load in line with the slow axis reduced the birefringence of the fibre by decreasing the effective refractive index in the slow axis. The corresponding strain in the fast axis increases its effective refractive index, thus lowering the birefringence as in [6], with a concomitant decrease in the wavelength separation of the two modes.

Results: The FBG feedback was observed to reduce the laser threshold to 16 mA, a reduction of 46%. The spectrum was observed using an Ando AQ-6310b optical spectrum analyser with a resolution of 0.1 nm. Fig. 1 shows the relative intensity of each mode during rotation of the wave plate, where the laser can be seen to switch the wavelength and polarisation of its output. The laser operated in three states, in states A and C the laser operated in a single longitudinal mode, orthogonally polarised for each state. In state B both orthogonally linearly polarised modes coexist, since the eigenaxes of the fibre are equally populated. The laser was seen to be mode hop free in all three states and temperature tuning of the diode could be used to ensure the switchable modes were of equal intensity. No mode or intensity instabilities were seen over a period of several hours. The wavelength separation of the two modes was 0.3 nm, which matches the separation expected from a FBG written in Hi-Bi fibre with a beat length of 1.6 mm at 810 nm. Fig. 2 shows the dependence of the lasing wavelengths upon the transverse load applied to the FBG, with the orientation of the fibre and direction of transverse load also shown. Loads of up to 0.34 N/mm were applied to the fibre, and a linear dependence of the wavelength separation upon the load was observed. These loads can be increased to increase the range over which the wavelength separation can be tuned.

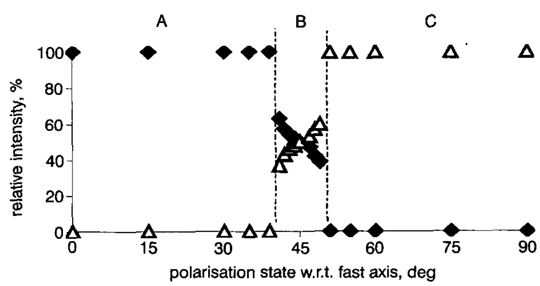

Fig. 1 *Relative intensity of orthogonally polarised modes as polarisation is rotated*

◆ fast axis mode
Δ slow axis mode

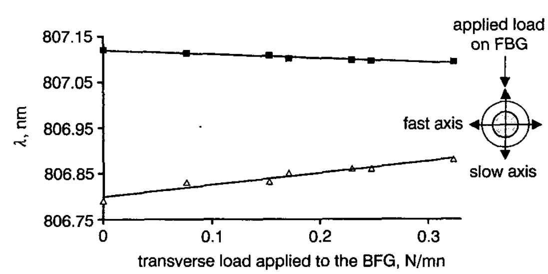

Fig. 2 *Dependence of lasing wavelengths upon applied transverse load (direction of transverse load application to fibre also indicated)*

Two-FBG lasers: The second laser configuration employs two spatially separated FBGs. The FBGs were fabricated in singlemode fibre at two different wavelengths, forcing the laser to lase on two longitudinal modes. As the two FBGs were not co-located, strain could be applied independently to each FBG, making both modes independently tunable. The interference between these two modes can be used to create a beat signal, the frequency of which is a function of